# Hierarchical Fast-Slow Singularly Perturbed Nonlinear Control: Application to Soft Multisection Robot Arms.

***Abstract*—**

**Supplementary material—All codes for reproducing the experiments reported in this paper are available online: https://github.com/robotsorcerer/dcm.**

## I. Introduction

Soft robots are finding wide adoption in automation needs owing to their configurability and compliance. These properties enable customizable solutions for assistive wearable devices [14, 1], robot grippers [6], and mobile robots [7]. Controlling these compliant robot manipulators (or actuators) remains a challenging task for real-time deployment. This is in part due to the long time-scales required to accurately compute models of their infinite-dimensional fibers in position- and velocity control schemes [8]. To meet copacetic system requirements, the practicing roboticist must wend a strait and narrow path — balancing the trade-off among high-fidelity models, (robust) asymptotically stable control, and the long transients of computing (kinematic/kinetic) solutions.

In the explicit and learning-based control regimes, the long computational times characteristic of closing the loop to zero steady-state offsets [8] often hampers real-time deployment efficacy in critical automation tasks. This is despite promising piecewise constant strain discretization techniques leveraging Cosserat rod theory [12] that provide better modeling accuracy for specialized bending motions. Even quasi-static modeling tools leveraging morphoelastic rod theory [9] possess restrictive assumptions that limit the deformable material configuration upon which these optimization tools can be applied [3, 4].

## II. Notations and Preliminaries

Time variables e.g. $t, T$, will always be real numbers. Conventions: Matrices and vectors are respectively upper- and lower-case Roman letters. Exceptions: the strain field and strain twist vectors are Greek letters, that is $\eta \in \mathbb{R}^6$ and $\xi \in \mathbb{R}^3$, respectively. Sets, screw stiffness, wrench tensors, and the gravitational vector are upper-case Calligraphic characters. Distributed wrench tensors are signified with an overbar, e.g. $\bar{\mathcal{F}}$. At a time $t$ and for a curve which is the material abscissa $X : [0, L]$[1], the robot's configuration is $\mathcal{X}_t(X)$. The matrix $A$'s Frobenius norm is denoted $\|A\|$ while its Euclidean norm is $\|A\|_2$. The Lie algebra of the Lie group $\mathbb{SE}(3)$ is $\mathfrak{se}(3)$. The special orthogonal group consisting of corkscrew rotations is $SO(3)$. For a configuration $\boldsymbol{g}(X) \in \mathbb{SE}(3)$, its adjoint and coadjoint are respectively $\mathrm{Ad}_{\boldsymbol{g}}$, $\mathrm{Ad}^{\star}_{\boldsymbol{g}}$; these are parameterized by the curve, $X$. In generalized coordinate, the joint vector of a soft robot is denoted $q = [\xi_1^\top, \ldots, \xi_{n_\xi}^\top]^\top \in \mathbb{R}^{6n_\xi}$.

Microsoft Research NYC lekanmolu@microsoft.com.

[1] $L$ is length of the curve.

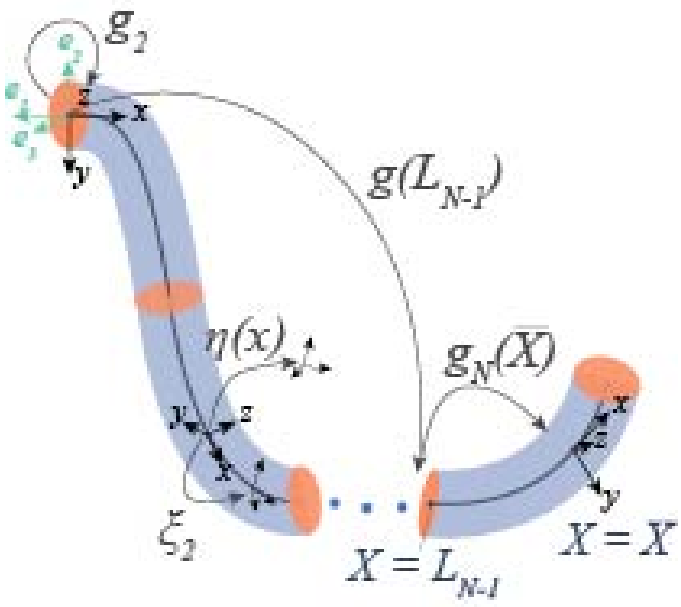


Fig. 1. Configuration schematic of an Octopus robot arm.

### A. SoRo Configuration

Depicted in Fig. 1, the inertial frame is the basis triad $(\boldsymbol{e}_1, \boldsymbol{e}_2, \boldsymbol{e}_3)$ and $\boldsymbol{g}_r$ is the inertial to base frame transformation. For a cable-driven arm, the point at which actuation occurs is labeled $\bar{X}$. The configuration matrix that parameterizes curve $L_n$ in $X$ is denoted $\boldsymbol{g}_{L_n}$. The cable runs through the $z$-axis (x-axis in the spatial frame) in the (micro) body frame.

### B. Continuous Strain Vector and Twist Velocity Fields

Suppose that $p(X) \in \mathbb{R}^6$ describes a microsolid's position on the soft body at $t$ and let $R(X)$ be the corresponding orientation matrix. Let the pose be $[p(X), R(X)]$. Then, the robot's C-space, parameterized by a curve $g(\cdot) : X \to \mathbb{SE}(3)$, is $g(X) = \begin{pmatrix} R(X) & p(X) \\ \mathbf{0}^\top & 1 \end{pmatrix}$. Suppose that $\varepsilon(X) \in \mathbb{R}^3$ and $\gamma(X) \in \mathbb{R}^3$ respectively denote the linear and angular strain components of the soft arm. Then, the arm's strain field is a state vector, $\breve{\xi}(X) \in \mathfrak{se}(3)$, along the curve $\boldsymbol{g}(X)$

i.e. $\breve{\xi}(X) = \boldsymbol{g}^{-1}\partial g/\partial X \triangleq \boldsymbol{g}^{-1}\partial_x \boldsymbol{g}$. In the microsolid frame, the matrix and vector representation of the strain state are respectively $\breve{\xi}(X) = \begin{pmatrix} \hat{\gamma} & \varepsilon \\ \mathbf{0} & 0 \end{pmatrix} \in \mathfrak{se}(3), \quad \xi(X) = \begin{pmatrix} \gamma^\top & \varepsilon^\top \end{pmatrix}^\top \in \mathbb{R}^6$. Read $\hat{\gamma}$: the anti-symmetric matrix representation of $\gamma$. Read $\breve{\xi}$: the isomorphism mapping the twist vector, $\xi \in \mathbb{R}^6$, to its matrix representation in $\mathfrak{se}(3)$. Furthermore, let $\nu(X), \omega(X)$ respectively denote the linear and angular velocities of the curve $g(X)$. Then, the velocity of $\boldsymbol{g}(X)$ is the twist vector field $\breve{\eta}(X) = \boldsymbol{g}^{-1}\partial \boldsymbol{g}/\partial t \triangleq \boldsymbol{g}^{-1}\partial_t \boldsymbol{g}$. In the microsolid frame, $\breve{\eta}(X) = \begin{pmatrix} \hat{\omega} & \nu \\ \mathbf{0} & 0 \end{pmatrix} \in \mathfrak{se}(3), \quad \eta(X) = \begin{pmatrix} \omega^\top & \nu^\top \end{pmatrix}^\top \in \mathbb{R}^6$.

### C. Discrete Cosserat-Constitutive PDEs

The PCS model assumes that $(\xi_i, \eta_i)\ i = 1, \ldots, N$ robot sections are constant. Spatially spliced along sectional boundaries, the overall strain position and velocity of the entire soft robot is a piecewise sum of the sectional strain field parameters.

Using d'Alembert's principle, the generalized dynamics equation for PCS model of Fig. 1 under external and actuation loads admits the form [12]

$$\underbrace{\left[\int_0^{L_N} J^\top \mathcal{M}_a J dX\right]}_{M(q)} \ddot{q} + \underbrace{\left[\int_0^{L_N} J^\top \mathrm{ad}^\star_{J\dot{q}} \mathcal{M}_a J dX\right]}_{C_1(q,\dot{q})} \dot{q} + \underbrace{\left[\int_0^{L_N} J^\top \mathcal{M}_a \dot{J} dX\right]}_{C_2(q,\dot{q})} \dot{q} + \underbrace{\left[\int_0^{L_N} J^\top \mathcal{D} J \|J\dot{q}\|_p dX\right]}_{D(q,\dot{q})} \dot{q} - \underbrace{(1-\rho_f/\rho)\left[\int_0^{L_N} J^\top \mathcal{M} \mathrm{Ad}^{-1}_{\boldsymbol{g}} dX\right]}_{N(q)} \mathrm{Ad}^{-1}_{\boldsymbol{g}_r}\mathcal{G} - \underbrace{J^\top(\bar{X})\mathcal{F}_p}_{F(q)} - \underbrace{\int_0^{L_N} J^\top \left[\nabla_x \mathcal{F}_i - \nabla_x \mathcal{F}_a + \mathrm{ad}^\star_{\eta_n}(\mathcal{F}_i - \mathcal{F}_a)\right] dX}_{\tau(q)} = 0 \tag{1}$$

for a Jacobian $J(X)$, (see definition in [12]), wrench of internal forces $\mathcal{F}_i(X)$, distributed wrench of actuation loads $\bar{\mathcal{F}}_a(X)$, and *distributed* wrench of the applied external forces $\bar{\mathcal{F}}_e(X)$. The torque and (internal) force are respectively $M_k, F_k$ for sections $k$; and $\mathcal{M}(X)$ is the screw mass inertia matrix, given as $\mathcal{M}(X) = \mathrm{diag}\,(I_x, I_y, I_z, A, A, A)\,\rho$ for a body density $\rho$, sectional area $A$, bending, torsion, and second inertia operator $I_x, I_y, I_z$ respectively.

Equation (1) can be appropriately written in standard Newton-Euler (N-E) form as

$$M(q)\ddot{q} + [C_1(q,\dot{q}) + C_2(q,\dot{q})]\,\dot{q} = \tau(q) + F(q) + N(q)\mathrm{Ad}^{-1}_{\boldsymbol{g}_r}\mathcal{G} - D(q,\dot{q})\dot{q}. \tag{2}$$

In (1), $\mathcal{M}_a = \mathcal{M} + \mathcal{M}_f$ is a lumped sum of the microsolid mass inertia operator, $\mathcal{M}$, and that of the added mass fluid, $\mathcal{M}_f$; $dX$ is the length of each section of the multi-robot arm; $\mathcal{D}(X)$ is the drag fluid mass matrix; $J(X)$ is the Jacobian operator; $\|\cdot\|_p$ is the translation norm of the expression contained therein; $\rho_f$ is the density of the fluid in which the material moves; $\rho$ is the body density; $\mathcal{G}$ is the gravitational vector defined as $\mathcal{G} = [0, 0, 0, -9.81, 0, 0]^T$; and $\mathcal{F}_p$ is the applied wrench at the point of actuation $\bar{X}$. These terms form the overall mass $M(q)$, Coriolis forces $C_i(q,\dot{q}), i = 1, 2$, buoyancy-gravitational forces $N(q)$, drag matrix $D(q,\dot{q})$ and external force $F(q)$ in (2).

Suppose that

$$z = \begin{pmatrix} z_1 & z_2 \end{pmatrix}^\top \equiv \begin{pmatrix} q & \dot{q} \end{pmatrix}^\top \tag{3}$$

then we may transform (2) into the following set of first-order differential equations

$$\dot{z}_1 = z_2, \tag{4a}$$

$$\dot{z}_2 = M^{-1}\left\{\tau - (C_1 + C_2 + D)z_2 + F + N\mathrm{Ad}^{-1}_{\boldsymbol{g}_r}\mathcal{G}\right\}, \tag{4b}$$

where we have omitted the templated arguments for simplicity. We refer readers to Renda et al. [12], Boyer and Renda [2], Renda et al. [11] for further details.

## III. Hierarchical Control Scheme

Our goal is to design a *multi-resolution feedback control scheme* which steer an arbitrary point in the joint space, $q(t)$ at time $t$, to a target point $q^d = (q_1^d, \ldots, q_N^d)^\top$[2] based on backstepping design for controlling underwater and terrestrial-based soft manipulators. Owing to the long computational times required to realize effective control [8], we shall transform the Cosserat system into a singularly perturbed system. Under standard singular perturbation theory (SPT) assumptions, we take a composite control system viewpoint — separating fast and slow dynamics as we decompose (2) into a nonlinear two time-scale system comprising separate fast and slow controllers.

### A. Singularly Perturbed Composite Backstepping Controller

For the soft manipulator of Fig. 1, the seemingly parsimonious PCS Newton-Euler dynamics (2) proves computationally burdensome to implement owing to the multiple integration time steps that gets adaptively executed when solving for control [8].

Seeking a robust response to parametric variations, noise sensitivity, and parasitic "small" time constants components of the dynamics that increase model order, we separate the fast- from low-changing dynamics. In the standard two-time-scale singular perturbation model, we separate the states of (2) into slow (i.e. $z_1$) and fast components (i.e. $z_2$) where asymptotic expansions of the high-dimensional system (2) into reduced slow and boundary-layer series allows for time-efficient control. Thus, we write

$$\dot{z}_1 = f(z_1, z_2, \epsilon, u_s, t),\ z_1(t_0) = z_1(0),\ z_1 \in \mathbb{R}^{6N} \tag{5a}$$

$$\epsilon\dot{z}_2 = h(z_1, z_2, \epsilon, u_f, t),\ z_2(t_0) = z_2(0),\ z_2 \in \mathbb{R}^{6N} \tag{5b}$$

where $f$ and $h$ are $\mathcal{C}^n (n \gg 0)$ differentiable functions of their arguments, $\epsilon > 0$ denotes all small parameters to be

[2]Here, $q_i$ is the joint space for a section of the multisection manipulator.

ignored[3], $u_s$ is the slow sub-dynamics' control law, and $u_f$ is the fast sub-dynamics' controller.

### B. Slow and Fast Subsystems Extraction

Let us set $\epsilon = 0$; this reduces the system's dimension so that (5b) becomes the algebraic equation

$$0 = h(\bar{z}_1, \bar{z}_2, 0, u_s, t) \tag{6}$$

where $\bar{(\cdot)}$ signifies a variable in the system with $\epsilon = 0$. We proceed with the following assumptions.

*Assumption 1 (Real and distinct root):* Equation (6) has a unique and distinct root, given as

$$\bar{z}_2 = \phi(\bar{z}_1, t). \tag{7}$$

Substituting (7) into (6), we have the form

$$0 = h(\bar{z}_1, \phi(\bar{z}_1, t), 0, u_s, t) \triangleq \bar{h}(\bar{z}_1, u_s, t), \;\; \bar{z}_1(t_0) = z_1(0), \tag{8}$$

where we have chosen the initial condition of the original system. Thus, the *quasi steady-state* (or slow) subsystem is

$$\dot{\bar{z}}_1 = f(\bar{z}_1, \bar{h}(\bar{z}_1, u_s, t), 0, u_s, t) \triangleq f_s(\bar{z}_1, u_s, t). \tag{9}$$

The slow (9) and original system's (5) transient response's variation constitutes the fast transient $\sigma = z_2 - \bar{h}(\bar{z}_1, u_s, t)$ on a time scale $T = t/\epsilon$ so that

$$\frac{dz_1}{dT} = \epsilon f(z_1, z_2, \epsilon, u_s, t), \tag{10a}$$

$$\begin{aligned}\frac{d\sigma}{dT} &= \epsilon \frac{dz_2}{dt} - \epsilon \frac{\partial \bar{h}_1}{\partial \bar{z}_1} \dot{\bar{z}}_1, \\ &= h(z_1, \alpha + \bar{h}(\bar{z}_1, u_s, t), \epsilon, u_f, t) - \epsilon \frac{\partial \bar{h}_1}{\partial \bar{z}_1} \dot{\bar{z}}_1.\end{aligned} \tag{10b}$$

When $\epsilon = 0$, for the fast subsystem we must have

$$\frac{d\sigma}{dT} = h(z_1, \sigma + \bar{h}(\bar{z}_1, u_s, t), 0, u_f, t). \tag{11}$$

### C. Singularly Perturbed SoRo Dynamics

First, we consider a cable-actuated robot. At point $\bar{X}$ (see Fig. 1) in a configuration $\mathcal{X}_t(\bar{X})$, the robot's motion around $\mathcal{X}_t(\bar{X})$ is a consequence of nearby micoroslids' deformation around configuration $\mathcal{X}_t(\bar{X})$. Denote the composite mass of these microsolids responsible for the core robot deformation as $\mathcal{M}^{\text{core}} = \oplus\{\mathcal{M}_1, \cdots, M_{\bar{n}}\}$[4]. The motion of every other microsolid (with mass $\mathcal{M}^{\text{pert}}$) is considered a perturbation from that of the motion of microsolids with mass $\mathcal{M}^{\text{core}}$ so that $\mathcal{M}^{\text{pert}} = \mathcal{M} \setminus \mathcal{M}^{\text{core}}$.

For fluid-driven robots such as fiber reinforced elastomeric enclosures (FREEs) with deformable shells [10], principal motion are a consequence of shell deformation (with core mass, $\mathcal{M}^{\text{core}}$) and $\mathcal{M}^{\text{pert}}$ constitutes the mass of remnant micro-solids apart from the deformable shell. The term $\mathcal{M}$ shows up in every integral term that make up the matrices $M(q)$, $C_1(q, \dot{q})$, $C_2(q, \dot{q})$ and $N(q)$ in (1). Ideally, we want to separate the slow and fast portions of the distributed components of the respective matrices $M(q)$, $C_1(q, \dot{q})$, $C_2(q, \dot{q})$ and $N(q)$ using different perturbation parameter values. However, on a closer observation of these matrices, we see that they have in common the distributed mass densities $\mathcal{M}^{\text{core}}$ and $\mathcal{M}^{\text{pert}}$. This allows us to choose a uniform perturbation parameter, $\epsilon = \|\mathcal{M}^{\text{core}}\|/\|\mathcal{M}^{\text{pert}}\|$, that accounts for the time-scale separation. This leads us to the following assumption.

*Assumption 2 (Uniform Perturbation Parameter):* A single perturbation parameter, $\epsilon$, is enough to render an *approximately* uniform decomposition of the mass-integro densities $M(q)$, $C_1(q, \dot{q})$, $C_2(q, \dot{q})$ and $N(q)$ in (1) since the essential mass density of the robot $\mathcal{M}^{\text{core}}$ is a component of their integrands as seen in (1).

Let the concerned matrix densities be separable as follows

$$M(q) = M^c(q) + M^p(q), \tag{12a}$$

$$C_k(q, \dot{q}) = C_k^c(q, \dot{q}) + C_k^p(q, \dot{q}), \tag{12b}$$

$$N(q) = N^c(q) + N^p(q), \tag{12c}$$

where $k = 1, 2$; and $(\cdot)^c, (\cdot)^p$ respectively denote the core and perturbed matrices over abscissa indices $[L^c_{\min}, L^c_{\max}]$ and $[L^p_{\min}, L^p_{\max}]$, respectively. Given the robot configuration shown in Fig. 1, we choose $0 \leq L^p_{\min} < L^c_{\min}$ and $L^c_{\max} < L^p_{\max} \leq L$. We write the singularly perturbed form of (4) as

$$\dot{z}_1 = z_2, \tag{13a}$$

$$\begin{aligned}\epsilon M \dot{z}_2 = \tau(z_1) + F(z_1) + N(z_1)\text{Ad}_{\boldsymbol{g}_r}^{-1}\mathcal{G} - \\ [C_1(z_1, z_2) + C_2(z_1, z_2) + D(z_1, z_2)]\, z_2.\end{aligned} \tag{13b}$$

The justification for this model is described in what follows.

*1) Quasi steady-state sub-dynamics extraction:* Following the arguments in the foregoing, on the perturbed microsolids deformation is minute so that the strain twists and acceleration dynamics i.e. $(\dot{z}_1, \dot{z}_2)$ are equally small. Thus, for the slow subdynamics (4) transforms into

$$\dot{z}_1 = z_2, \tag{14a}$$

$$\begin{aligned}\epsilon M^p(z_1)\dot{z}_2 = \tau(z_1) + F(z_1) + N^p(z_1)\text{Ad}_{\boldsymbol{g}_r}^{-1}\mathcal{G} - \\ [C_1^p(z_1, z_2) + C_2^p(z_1, z_2) + D(z_1, z_2)]\, z_2.\end{aligned} \tag{14b}$$

For $\epsilon = 0$, the resulting algebraic equation is

$$\begin{aligned}\tau(\bar{z}_1) + F(\bar{z}_1) + N^p(\bar{z}_1)\text{Ad}_{\boldsymbol{g}_r}^{-1}\mathcal{G} - \\ [C_1^p(\bar{z}_1, \bar{z}_2) + C_2^p(\bar{z}_1, \bar{z}_2) + D(\bar{z}_1, \bar{z}_2)]\, \bar{z}_2 = 0\end{aligned} \tag{15}$$

so that

$$\begin{aligned}\bar{z}_2 = [C_1^p(\bar{z}_1, \bar{z}_2) + C_2^p(\bar{z}_1, \bar{z}_2) + D(\bar{z}_1, \bar{z}_2)]^{-1} \{\tau(\bar{z}_1) \\ + F(\bar{z}_1) + N(\bar{z}_1)\text{Ad}_{\boldsymbol{g}_r}^{-1}\mathcal{G}\}\end{aligned} \tag{16}$$

where the bar signifies variables within the reduced system. Thus, the slow subsystem can be written as

$$\begin{aligned}\dot{\bar{z}}_1 = \bar{z}_2, \\ \triangleq [C_1^p(\bar{z}_1, \bar{z}_2) + C_2^p(\bar{z}_1, \bar{z}_2) + D(\bar{z}_1, \bar{z}_2)]^{-1} \{\tau(\bar{z}_1) \\ + F(\bar{z}_1) + N(\bar{z}_1)\text{Ad}_{\boldsymbol{g}_r}^{-1}\mathcal{G}\}\end{aligned} \tag{17}$$

[3]Restriction to a two-time-scale is not binding and one can choose to expand the system into multiple sub-dynamics across multiple time scales.

[4]where $\bar{n} < n$ and $\oplus$ operator implies an arithmetic sum of the respective elements of the set.

*2) Fast subsystem dynamics extraction:* The residual of the original system from the slow subsystem i.e. $\tilde{z}_2 = z_2 - \bar{z}_2$ is the fast transient on a time scale $T = t/\epsilon$. Whence, the fastest subsystem's dynamics evolves as

$$\frac{dz_1}{dT} = \epsilon z_2, \quad T = t/\epsilon, \tag{18a}$$

$$(M^c(z_1) + \epsilon\Lambda_m)\frac{d\tilde{z}_2}{dT} = \tau(z_1) + F(z_1) + (N^c(z_1) + \epsilon\Lambda^n)\mathrm{Ad}_{\boldsymbol{g}_r}^{-1}\mathcal{G} - (C_1^c + \epsilon\Lambda_1^c + C_2^c + \epsilon\Lambda_2^c + D)\, z_2 \tag{18b}$$

where we have occasionally omitted the templated arguments for ease of notation, and $\Lambda^m = M^p/\epsilon$, $\Lambda_1^c = C_1^p/\epsilon$, $\Lambda_2^c = C_2^p/\epsilon$, $\Lambda^n = N^p/\epsilon$, $\epsilon = \|\mathcal{M}^{\text{core}}\|/\|\mathcal{M}^{\text{pert}}\|$, and the matrix $(M^c + \epsilon\Lambda_m)$ is assumed to be invertible. Carrying out the standard $\epsilon = 0$ on the fast time scale, we find that

$$\frac{dz_1}{dT} = 0, \tag{19a}$$

$$M^c(z_1)\frac{d\tilde{z}_2}{dT} = \tau(z_1) + F(z_1) + N^c(z_1)\mathrm{Ad}_{\boldsymbol{g}_r}^{-1}\mathcal{G} - [C_1^c(z_1,\tilde{z}_2) + C_2^c(z_1,\tilde{z}_2) + D(z_1,\tilde{z}_2)]\,\tilde{z}_2. \tag{19b}$$

### D. Control and Stability Analyses

We proceed to design nonlinear backstepping controllers for the two separate time-scale problems developed in §III-C. We then address the global asymptotic stability of the singularly perturbed system (13) with Lyapunov analysis using standard comparison functions [5]. The reduced and boundary layer systems of interest are

$$\frac{d\bar{z}_1}{dt} = [C_1^p(\bar{z}_1,\bar{z}_2) + C_2^p(\bar{z}_1,\bar{z}_2) + D(\bar{z}_1,\bar{z}_2)]^{-1}\{\tau(\bar{z}_1) + F(\bar{z}_1) + N(\bar{z}_1)\mathrm{Ad}_{\boldsymbol{g}_r}^{-1}\mathcal{G}\}, \tag{20a}$$

$$M^c(z_1)\frac{d\tilde{z}_2}{dT} = \tau(z_1) + F(z_1) + N^c(z_1)\mathrm{Ad}_{\boldsymbol{g}_r}^{-1}\mathcal{G} - [C_1^c(z_1,\tilde{z}_2) + C_2^c(z_1,\tilde{z}_2) + D(z_1,\tilde{z}_2)]\,\tilde{z}_2 \tag{20b}$$

where $z_1$ is fixed in (20b).

*Assumption 3 (**Solution assumptions**):* We make the following assumptions about Lyapunov function candidates for the reduced (17), boundary layer (19), and the full singularly perturbed system (13).

- For all $t \geq 0$, $z_1(t) \in S$ where $S$ is a compact subset of $\mathbb{R}^{6N}$. This assures that $z_1(t)$ remains bounded as $t \to \infty$;
- The origin of (13) is an isolated equilibrium in $\mathbb{R}^{6N} \times \mathbb{R}^{6N}$ i.e.

$$0 = z_2, \tag{21a}$$

$$0 = \tau(0) + F(0) + N(0)\mathrm{Ad}_{\boldsymbol{g}_r}^{-1}\mathcal{G}; \tag{21b}$$

  and
- $z_2 = h(z_1)$ is a unique root of (21b) where $h(z_1)$ is a sufficiently many times continuously differentiable function of $z_1$.

Let us now consider comparison inequalities imposed on the Lyapunov functions of the slow and fast subdynamics respectively.

*Assumption 4 (Boundary Layer's Lyapunov Candidate):* The boundary layer system (19) admits a Lyapunov function candidate $W(z_1, z_2)$ (whereupon $z_1$ is treated as a fixed parameter) such that for all $(z_1, z_2) \in \mathbb{R}^{6N} \times \mathbb{R}^{6N}$, the following holds

(i) $W(z_1, z_2) > 0 \;\forall\; z_2 \neq h(z_1)$ and $W(z_1, \bar{z}_2)) = 0$,

(ii) $\dfrac{\partial W}{\partial z_1}\dot{z}_1 \leq \gamma\phi^2(z_2 - \bar{z}_2) + \beta_2\psi(z_1)\phi(z_2 - \bar{z}_2)$,

(iii) $\dfrac{\partial W}{\partial z_2}\dot{z}_2 \leq -\dfrac{1}{\epsilon}\alpha_2 M^{-1}\phi^2(z_2 - \bar{z}_2), \quad \alpha_2 > 0$,

where $\psi(z_1)$ and $\phi(\cdot)$ are scalar functions which vanish when their vector arguments are zero; and $\gamma$ and $\beta_2$ can be positive, zero, or negative. Note that the condition (ii) above implies that $\bar{z}_2$ is an origin (this also follows from (21a)).

*Assumption 5 (Slow subsystem's Lyapunov Candidate):* Let us rewrite (13a) as

$$\dot{z}_1 = \bar{z}_2 + z_2 - \bar{z}_2 \tag{22}$$

where $z_2 - \bar{z}_2$ is the reduced system (9)'s perturbation. Let a Lyapunov function candidate $V(z_1)$ exist so that the following inequality

$$\frac{\partial V}{\partial z_1}\dot{\bar{z}}_1 \leq -\alpha_1\psi^2(z_1) \quad \alpha_1 > 0, \tag{23}$$

assures that $\bar{z}_1 = 0$ is an asymptotically stable equilibrium. Then,

$$\frac{\partial V}{\partial z_1}\dot{z}_1 = \frac{\partial V}{\partial z_1}\dot{\bar{z}}_1 + \frac{\partial V}{\partial z_1}(\dot{z}_1 - \dot{\bar{z}}_1) \leq -\alpha_1\psi^2(z_1) + \frac{\partial V}{\partial z_1}(z_2 - \bar{z}_2). \tag{24}$$

If we prescribe the growth of $\dot{z}_1$ in $\bar{z}_2$ by $\dfrac{\partial V}{\partial z_1}(z_2 - \bar{z}_2) \leq \beta_1\psi(z_1)\phi(z_2 - \bar{z}_2)$, then

$$\dot{V} \leq -\alpha_1\psi^2(z_1) + \beta_1\psi(z_1)\phi(z_2 - \bar{z}_2). \tag{25}$$

*Assumption 6 (Global Lyapunov Function Candidate):* Given assumptions 4 and 5, there exists a convex combination of the separate Lyapunov functions which can be prescribed for the singularly perturbed system (12) as

$$\Lambda(z_1, z_2) = (1 - \sigma)V(z_1) + \sigma W(z_1, z_2), \; 0 < \sigma < 1, \tag{26}$$

Along the trajectories of (12), it follows that

$$\begin{aligned}\frac{d\Lambda}{dt} &= (1-\sigma)\frac{\partial V}{\partial z_1}\dot{z}_1 + \frac{\sigma}{\epsilon}\frac{\partial W}{\partial z_1}\dot{z}_1 + \sigma\frac{\partial W}{\partial z_2}\dot{z}_2 \\ &= (1-\sigma)\left[\frac{\partial V}{\partial z_1}\dot{\bar{z}}_1 + \frac{\partial V}{\partial z_1}(\dot{z}_1 - \dot{\bar{z}}_1)\right] + \frac{\sigma}{\epsilon}\frac{\partial W}{\partial z_1}\dot{z}_1 + \sigma\frac{\partial W}{\partial z_2}\dot{z}_2 \\ &\leq (1-\sigma)\left[\alpha_1\psi^2(z_1) - \beta_1\psi(z_1)\phi(z_2 - \bar{z}_2)\right] + \frac{\sigma}{\epsilon}\left[\gamma\phi^2(z_2 - \bar{z}_2) + \beta_2\psi(z_1)\phi(z_2 - \bar{z}_2) - \epsilon\alpha_2 M^{-1}\phi^2(z_2 - \bar{z}_2)\right]\end{aligned} \tag{27, 28}$$

### E. Nominal Backstepping Controller

Here, we consider a Lyapunov control redesign formulation using the discretized Cosserat Newton-Euler model (2). We seek a new representation of the PCS equation (2) by choosing a virtual variable $\eta(\xi(t))$ in the form of a feedback control variable. We backstep this through a system integrator by augmenting a control Lyapunov function (CLF) for reparameterized (2) with a quadratic error term so that altogether we arrive at an exponentially stable system. Let us proceed.

Consider the subsystem $\dot{z}_1 = \nu_1$ where $\nu_1$ is a virtual input. Let $q_d(t) \in \mathbb{R}^{6N}$ denote the reference trajectory for $z_1(t)$ to track and let the tracking error be $e_1 = z_1 - q^d$. We propose the Lyapunov function candidate

$$V_1(q(t)) = \frac{1}{2} e_1^\top(q(t)) K_p e_1(q(t)) \tag{29}$$

where $K_p \in \mathbb{R}^{6N\times 6N}$ is a positive definite matrix so that

$$\dot{V}_1(q) = e_1^\top K_p \dot{e}_1 = e_1^\top K_p(\nu_1 - \dot{q}_d) \tag{30}$$

where we have dropped the templated arguments on the rhs. Next, set the virtual input as $\nu_1 = \dot{q}_d - e_1$ so that

$$\dot{V}_1(q) = -e_1^\top K_p e_1 \leq 0 \tag{31}$$

where equality is only achieved at $e_1 = 0$. That is, $\lim_{t\to\infty} e_1(t) = 0$ or $z_1(t)$ converges to the reference trajectory $q_d(t)$ asymptotically under the virtual input $\nu_1 = \dot{q}_d - e_1$.

Now, consider the full nonlinear system (4) and design a stabilizing controller $\tau$ for $z_1(t)$ to track $q_d(t)$ based on the virtual input $\nu_1$ and Lyapunov function $V_1(q)$. Define the error $e_2 = z_2 - \nu_1$ and we obtain

$$\dot{e}_1 = \dot{z}_1 - \dot{q}_d = z_2 - \dot{q}_d \triangleq e_2 - e_1, \tag{32a}$$
$$\dot{e}_2 = \dot{z}_2 - \dot{\nu}_1 = \dot{z}_2 - \ddot{q}_d + \dot{e}_1 \triangleq \dot{z}_2 - \ddot{q}_d + e_2 - e_1. \tag{32b}$$

For the Lyapunov function candidate

$$V(q) = V_1(q) + \frac{1}{2} e_2^\top M e_2 \triangleq \frac{1}{2} e_1^\top K_p e_1 + \frac{1}{2} e_2^\top M e_2, \tag{33}$$

the time derivative of $V$ is

$$\begin{aligned} \dot{V}(q) &= e_1^\top K_p \dot{e}_1 + e_2^\top M \dot{e}_2 + \frac{1}{2} e_2^\top \dot{M} e_2, \\ &\triangleq e_1^\top K_p(e_2 - e_1) + e_2^\top M \dot{e}_2 + \frac{1}{2} e_2^\top \dot{M} e_2. \end{aligned} \tag{34}$$

Let us parameterize the full controller as

$$\tau = M\dot{\nu}_1 + [C_1 + C_2]\nu_1 + Dz_2 - (F + N\mathrm{Ad}_{\boldsymbol{g}_r}^{-1}\mathcal{G}) + u, \tag{35}$$

where $u$ is the residual control input (to be designed). Plugging (35) into (4), we have

$$M\dot{e}_2 + (C_1 + C_2)e_2 = u(q, \dot{q}). \tag{36}$$

Then, (34) becomes

$$\begin{aligned} \dot{V}(q) &= e_1^\top K_p(e_2 - e_1) + e_2^\top M \dot{e}_2 + \frac{1}{2} e_2^\top \dot{M} e_2, \\ &= e_1^\top K_p(e_2 - e_1) + e_2^\top (u - (C_1 + C_2)e_2) + \frac{1}{2} e_2^\top \dot{M} e_2, \\ &= -e_1^\top K_p e_1 + \frac{1}{2} e_2^\top (\dot{M} - 2(C_1 + C_2))e_2 + e_2^\top (K_p e_1 + u). \end{aligned}$$

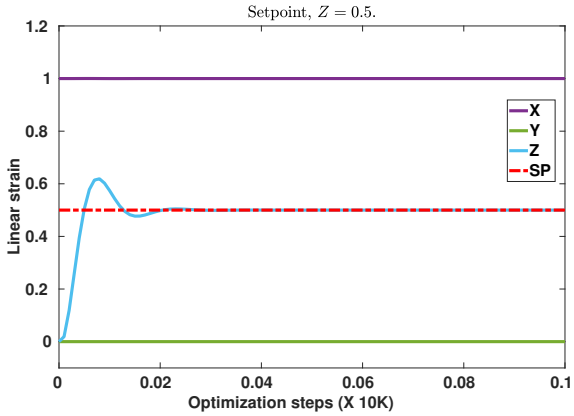


Fig. 2. Backstepping controller for $\xi = [0, 0, 0, 1, 0, 0.5]$.

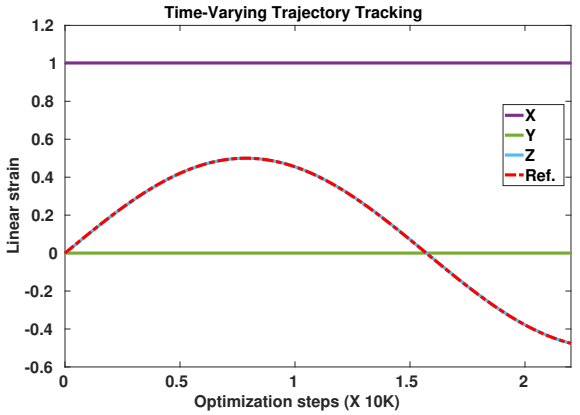


Fig. 3. Effect of nominal backstepping controller for a time-varying trajectory for a fixed strain about the $z$-axis of the local frame.

Let $u(q, \dot{q}) = -K_p e_1 - M(q)e_2$, then we must have

$$\dot{V}(q) = -e_1^\top K_p e_1 - e_2^\top M(q) e_2, \tag{37a}$$
$$\triangleq -2V. \tag{37b}$$

Thus, the Lyapunov function *guarantees exponential stability of trajectories* that emanate from the system under the control law (input torque)

$$\tau = M(\dot{\nu}_1 - e_2) + (C_1 + C_2)\nu_1 + Dz_2 - (F + N\mathrm{Ad}_{\boldsymbol{g}_r}^{-1}\mathcal{G}) - K_p e_1 \tag{38}$$

since $M(q)$ is positive definite and bounded from below as shown in [8]. Since $\dot{\nu}_1 = \ddot{q}_d - \dot{e}_1 = \ddot{q}_d - (e_2 - e_1)$, the controller in (38) can also be written as

$$\begin{aligned} \tau = M(q)(\ddot{q}_d - 2e_2 + e_1) + \breve{C}(q, \dot{q})(q_d - e_1) \\ + D(q)\dot{q} - F(q) - N(q)\mathrm{Ad}_{\boldsymbol{g}_r}^{-1}\mathcal{G} - K_p e_1, \end{aligned} \tag{39}$$

with

$$\breve{C}(q, \dot{q}) = C_1(q, \dot{q}) + C_2(q, \dot{q}), \tag{40a}$$
$$e_1 = q - q_d, \text{ and } e_2 = \dot{q} - \dot{q}_d + e_1. \tag{40b}$$

## IV. Numerical Results

## V. Discussions and Conclusion

## References


[1] Gunjan Agarwal, Nicolas Besuchet, Basile Audergon, and Jamie Paik. Stretchable Materials for Robust Soft Actuators Towards Assistive Wearable Devices. *Scientific reports*, 6(1):34224, 2016. 1

[2] Frederic Boyer and Federico Renda. Poincaré's equations for cosserat media: application to shells. *Journal of Nonlinear Science*, 2016. 2

[3] Bartosz Kaczmarski, Alain Goriely, Ellen Kuhl, and Derek E Moulton. A Simulation Tool for Physics-informed Control of Biomimetic Soft Robotic Arms. *IEEE Robotics and Automation Letters*, 8(2):936–943, 2023. 1

[4] Bartosz Kaczmarski, Derek E. Moulton, Alain Goriely, and Ellen Kuhl. Bayesian design optimization of biomimetic soft actuators. *Computer Methods in Applied Mechanics and Engineering*, 408:115939, 2023. ISSN 0045-7825. 1

[5] Hassan K Khalil. *Nonlinear Control*, volume 406. Pearson New York, 2015. 4

[6] Mariangela Manti, Taimoor Hassan, Giovanni Passetti, Nicolò D'Elia, Cecilia Laschi, and Matteo Cianchetti. A Bioinspired Soft Robotic Gripper for Adaptable and Effective Grasping. *Soft Robotics*, 2(3):107–116, 2015. 1

[7] Andrew D Marchese, Cagdas D Onal, and Daniela Rus. Autonomous Soft Robotic Fish Capable of Escape Maneuvers Using Fluidic Elastomer Actuators. *Soft robotics*, 1(1):75–87, 2014. 1

[8] Lekan Molu, James Forbes, and Audrey Sedal. The Discrete Cosserat Model for Piecewise Constant Strain Deformation, *Redux*. Structural Properties and Control. *(submitted to) Robotics and Automation Letters; IEEE International Conference on Robotics and Automation*, 2023. 1, 2, 5

[9] Derek E Moulton, Thomas Lessinnes, and Alain Goriely. Morphoelastic Rods III: Differential Growth and Curvature Generation in Elastic Filaments. *Journal of the Mechanics and Physics of Solids*, 142:104022, 2020. 1

[10] Olalekan Ogunmolu, Xinmin Liu, Nicholas Gans, and Rodney D Wiersma. Mechanism and model of a soft robot for head stabilization in cancer radiation therapy. In *2020 IEEE International Conference on Robotics and Automation (ICRA)*, pages 4609–4615. IEEE, 2020. 3

[11] Federico Renda, Vito Cacucciolo, Jorge Dias, and Lakmal Seneviratne. Discrete cosserat approach for soft robot dynamics: A new piece-wise constant strain model with torsion and shears. *IEEE International Conference on Intelligent Robots and Systems*, 2016-Novem:5495–5502, 2016. ISSN 21530866. 2

[12] Federico Renda, Frédéric Boyer, Jorge Dias, and Lakmal Seneviratne. Discrete cosserat approach for multi-section soft manipulator dynamics. *IEEE Transactions on Robotics*, 34(6):1518–1533, 2018. 1, 2

[13] Audrey Sedal, Daniel Bruder, Joshua Bishop-Moser, Ram Vasudevan, and Sridhar Kota. A continuum model for fiber-reinforced soft robot actuators. *Journal of Mechanisms and Robotics*, 10(2):024501, 2018.

[14] Hong Kai Yap, Nazir Kamaldin, Jeong Hoon Lim, Fatima A Nasrallah, James Cho Hong Goh, and Chen-Hua Yeow. A Magnetic Resonance Compatible Soft Wearable Robotic Glove for Hand Rehabilitation and Brain Imaging. *IEEE transactions on neural systems and rehabilitation engineering*, 25(6):782–793, 2016. 1